

Optical Studies of Undoped and Doped Wide Bandgap Carbide and Nitride Semiconductors

J.A. Freitas, Jr. and W.J. Moore

Naval Research Laboratory

4555 Overlook Ave, S.W.

Washington DC 20375-5347 USA

Received February 2, 1997

The wide bandgap semiconductors Silicon carbide and gallium nitride have been studied by Raman scattering, photoluminescence, and infrared absorption. Raman scattering studies determined crystalline quality and polytype of bulk and thin film samples at room temperature. Photoluminescence studies were carried out as a function of temperature to detect and/or identify impurity centers and structure related defects and their role on the electronic properties of the materials. Infrared absorption spectroscopy was used to measure the binding energy of donors and their concentration.

I. Introduction

The increasing need for electronic devices capable of performing under extreme condition of power and temperature and opto-electronic devices operating in the UV spectral range has been the principal driving force for the research interest in large bandgap materials over the last two decades.

Continuous progress in chemical vapor deposition (CVD) and molecular beam epitaxy (MBE) techniques for homo- and hetero-epitaxial growth of wide bandgap semiconductors has led to the successful fabrication and commercialization of an increasing number of devices using these materials. The high deposition temperature usually required for growth of these wide bandgap materials increases fundamental material problems such as residual strain, thermal expansion coefficient, low energy defect formation, and impurity incorporation. In addition, doping activation and self-compensation are difficult to control at high deposition temperatures. Full realization of the electronic and opto-electronic applications of large bandgap semiconductors requires understanding the role of incorporation and activation of unintentional and intentional impurities, and structural defects.

Significant recent advances in growth, doping, and processing technologies of SiC (3C, 4H and 6H polytypes) and III-V nitrides (AlN, GaN, AlGaIn, and In-

GaN alloys) indicate that these materials present important advantages for many areas of semiconductor electronics applications.

The evolution of the sublimation technique introduced by Lely in 1955 for the fabrication of α -SiC has made possible the fabrication of high quality bulk 4H- and 6H-SiC [1]. Homoepitaxial film deposition on such material wafers has been successfully used to fabricate high-power and high-frequency devices [2]. Unfortunately, such techniques have not yet been capable of producing high quality bulk 3C-SiC [3,4]. High quality and relatively small size bulk cubic SiC can be grown by atmospheric-pressure CVD on graphite substrates from methyltrichlorosilane [5,6]. However, the small size of these crystals precludes most practical applications. Large area heteroepitaxial 3C-SiC films have been deposited on {001} Si-substrates by the CVD technique [7-9]. These films are usually n-type with high donor concentrations and a debated acceptor concentration [10-12]. Optical and scanning electron microscopy (SEM) studies of such monocrystalline films have revealed high densities of lattice defects such as stacking faults and antiphase boundaries [13,14].

GaN crystals grown by the sublimation technique are needle shaped with average lengths less than 1 mm [15]. Thin GaN platelets (8 mm x 5 mm) have been grown from a solution of atomic nitrogen in liq-

uid Ga at N_2 pressure up to 20 kbar [16]. Although these platelets have good structural properties, their slow growth (0.1 mmh in $\{10\bar{1}0\}$ direction) and electronic properties are disadvantages in commercial application. Homoepitaxial films deposited on such platelets provide the baseline characterization for heteroepitaxial films [17]. Heteroepitaxial GaN films are routinely deposited on sapphire or 6H-SiC substrates despite the large lattice mismatch in thermal expansion coefficients and lattice parameters. Experimental evidence indicates that the biaxial strain is relieved by forming dislocations with a density typically between 10^8 cm^{-2} to 10^{10} cm^{-2} [18,19]. Although GaN devices with very good performance have been produced, the state of the art of these device is still material quality limited.

In the present work we describe the use of a combination of optical techniques to study native defects and dopants in cubic SiC (3C-SiC) and wurtzite GaN.

II. Experimental techniques

Films of 3C-SiC have been grown on Si(100) surfaces which have been chemically converted using a reaction reaction with C_2H_4 or C_3H_8 . This was followed by a chemical vapor deposition in which SiH_4 and C_2H_4 or C_3H_8 in H_2 are passed over the Si- substrate on a graphite susceptor at temperature between 1620 and 1670K [9].

Bulk 3C-SiC samples were grown on resistively heated graphite rods by decomposition of methyltrichlorosilane in a Hydrogen carrier gas at atmospheric pressure. At temperatures of about 1750°C hexagonally shaped $\{111\}$ -oriented light yellow platelets of 3 mm to 5 mm were obtained [5].

Undoped and doped GaN films were deposited on c-plane (basal plane) and or a-plane ($11\bar{2}0$) sapphire substrates using a low pressure metalorganic CVD system. To reduce the large lattice mismatch between the GaN film and the sapphire substrate a thin film of either AlN or GaN was deposited a low temperature followed by deposition of GaN at a temperature of about 1000°C . The Si-doped and Mg-doped films were deposited under similar conditions to those of the undoped films [20-22].

The Raman scattering (RS) and photoluminescence (PL) experiments used an Ar ion laser and a HeCd laser, respectively. The RS spectra presented here were obtained at room temperature, while the PL spectra were measured with the samples contained in a liquid Helium cryostat which provided temperatures ranging

from 1.5K to 330K. The light scattered and emitted by the samples was dispersed and analyzed by a double grating spectrometer fitted with a UV-sensitive GaAs photomultiplier operated in the photon counting mode.

The infrared (IR) transmission experiment was performed with samples packed into an aperture in a brass plate with pure In and mounted into a light pipe with a sample heater and a gallium-doped Ge photodetector. The entire assembly was cooled by immersion in liquid He. Infrared spectra were acquired with a Fourier transform spectrometer.

III. Phonons

The basic unit of SiC consists of a covalently bonded tetrahedron of Si (or C) with C (or Si) at the center. The identical polar layers of Si_4C (or C_4Si) are continuously stacked and the permutation of stacking sequences allows a large number of polytypes. The cubic SiC crystallizes in the zinc blend structure, which has two atoms per unit cell. The optical modes split into one non-degenerated longitudinal optical phonon (LO) and two degenerated transverse optical phonons (TO). The pure hexagonal polytype 2H, has the wurtzite structure and four atoms per unit cell. Consequently, it has nine long-wavelength optical modes. The following Raman active phonons can be observed near the center of the Brillouin Zone (BZ): an A_1 mode with polarization in the uniaxial direction, a doubly-degenerated E_1 mode in the plane perpendicular to the uniaxial direction, and two doubly degenerated E_2 modes.

The 4H- and 6H-SiC polytypes, commonly used for device fabrication, have 8 and 12 atoms per unit cell, respectively. Their larger unit cell results in a larger number of optical phonons than 3C- and 2H- SiC. One can use Raman spectra to identify the polytype structure [23]. Fig. 1 shows the Raman scattering spectrum of bulk 3C-, 4H-, and 6H-SiC polytypes. The number and observed frequencies of the spectral features in the Raman spectrum for cubic SiC are completely different and readily distinguishable from those of hexagonal material.

Cubic (zinc blend) and hexagonal (wurtzite) GaN can be deposited by CVD techniques. Since the cubic phase is less stable than the hexagonal phase, layers of cubic-GaN always present a large fraction of hexagonal component [24]. The hexagonal phase has two molecules in the unit cell. Therefore nine optical branches are expected, namely: $1A_1(\text{TO})$, $1A_1(\text{LO})$, $2B_1$, $1E_1(\text{TO})$, $1E_1(\text{LO})$, and $2E_2$. The two modes B_1

are optically inactive, but all the six allowed modes have been observed by Raman spectroscopy [25]. The RS spectrum of a 5.0 μm GaN film deposited on sapphire is presented in Fig. 2.

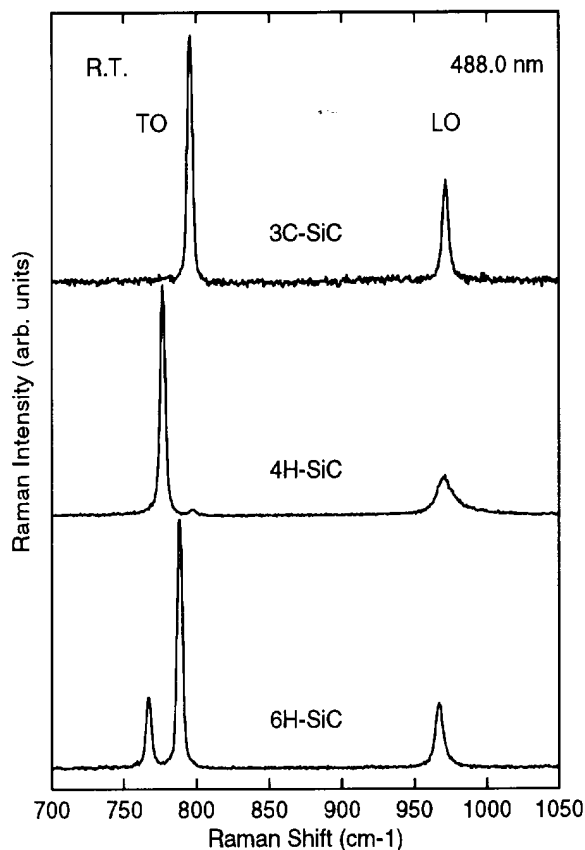


Fig. 1. Raman spectra of three SiC polytypes. Note that the 3C-SiC spectrum has two lines, while the 4H- and 6H-SiC polytypes spectra have three lines.

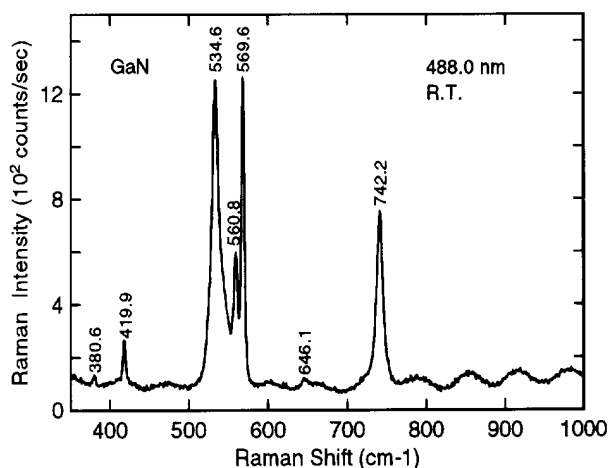


Fig. 2. Raman spectrum of an undoped GaN film on sapphire. The peaks at about 381 cm^{-1} , 420 cm^{-1} , 646 cm^{-1} , are due to the sapphire substrate.

IV. Donors

Low temperature optical absorption experiments performed on several SiC polytypes verify the indirect character of the band gap and provide a value for the exciton band gap [26]. The low temperature photoluminescence (LTPL) spectrum of undoped 3C-SiC, shown in Fig. 3, is characterized by a set of five intense sharp lines between 2.39 and 2.26 eV. The first line has been assigned to a recombination process involving the annihilation of excitons bound to neutral nitrogen donors ($X-N^{\circ}$). The other intense lines (marked as /TA, /LA, /TO, and /LO) are the momentum conserving recombination processes, as expected for an indirect gap material [27]. It is important to point out that the phonons represented here are those at the edge of the BZ and are therefore different from phonons at the center of the BZ which are observed by RS. The high quality of this sample is evident in these spectra not only in the sharpness of the observed lines (<0.1 meV), but also in the presence of multiple bound excitons ($2(X-N^{\circ})$ and $3(X-N^{\circ})$). Under higher laser excitation conditions we are able to observe lines associated with free-excitons and two-electron satellite recombinations [28]. The latter are a result of recombination processes in which the N° -donors are left in excited states after the exciton recombination. Because of a large number of phonons and multiple, inequivalent sites for the N- donor, the PL spectra of other SiC polytypes are significantly more complex.

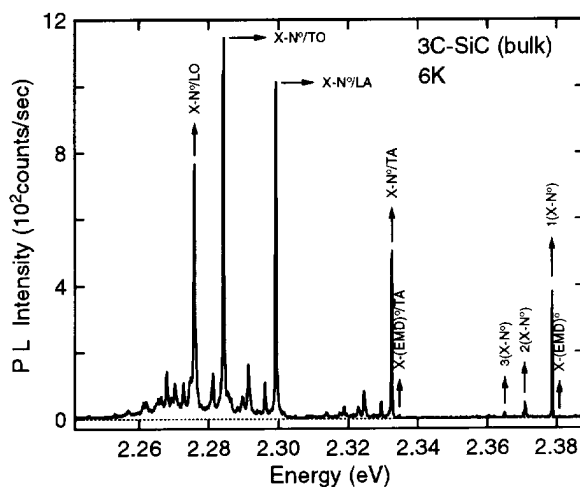


Fig. 3. Low temperature PL spectra of a bulk 3C-SiC sample. The 325 nm (3.81 eV) He-Cd laser line was used as exciting source.

LTPL spectra of cubic CVD films reproduce most of the features observed in the bulk spectra. The two-electron satellite spectrum is absent and exciton line widths in the films are usually about 20 times broader [29].

Infrared absorption experiments performed in our bulk samples at about 4.5 K reveal, in the spectral range between 25 to 55 meV, the presence of broad and sharp sequences of donor excitation transitions. We assign the broad sequence to transitions from the $1s(A_1)$ ground state of Nitrogen on the Carbon site (N_c) and the narrow sequence to transitions at an unidentified true effective mass donor (EMD) (Fig. 4). At higher temperatures we observe a second sequence of broad transitions, which we have attributed to $1s(E)$ ground state of the N_c . The energy separation between these two sequences, 8.4 meV, is the value of the valley-orbit splitting. We obtain 54.2 meV for the N_c binding energy, which is in excellent agreement with PL measurements (two electron satellite spectrum), and 47.8 meV binding energy for the EMD [30].

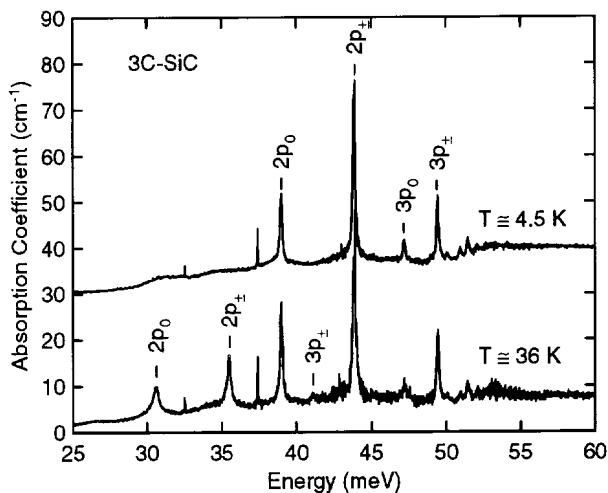


Fig. 4. 3C-SiC absorbance spectrum near 4.5 K (shifted up for clarity) and near 36 K. Note the difference between the broad (N_c) sequence and the sharp (EMD) sequence.

The PL spectra of undoped GaN heteroepitaxial films usually are dominated by a sharp emission at 3.47 eV and a broad featureless band peaking around 2.25 eV (yellow band). The former has been assigned to excitons bound to unidentified neutral donors, and the latter attributed to an unknown or carbon related defect [25,31]. Fabrication of undoped high resistivity ($\geq 10^{10} \Omega \text{ cm}$) and Si-doped material has been demonstrated over a wide range of concentration [22]. Al-

though we still observe the yellow emission band in the LTPL spectra of these films, the edge emission bands are quite different, as observed in Fig. 5. Note that the edge emission of the undoped/high resistivity (UHR) film is blue shifted and comprises a superposition of three individual bands at approximately 3.4867 eV, 3.4923 eV, and 3.5037 eV. Detailed temperature study supports our assignment of these individual bands to the ground state of free-exciton A (FE- A_1), the ground state of free-exciton B (FE- B_1), and the excited state of FE-A (FE- A_2), respectively [32]. Assuming an effective mass approximation, we estimate a value of 22.7 meV for the exciton binding energy based on a measured separation of 17 meV between the ground state and the excited state of the FE-A. We attribute the edge emission from the Si-doped sample to the annihilation of excitons bound to a neutral Si-donor, since this line is observed only in Si-doped samples [32]. The energy difference between the emission peaks in Si-doped and UHR films, 8.8 meV, is the value of the exciton binding energy to Si⁰-donor. This value is distinct from the 3 or 4 meV energy difference usually observed between the autodoped and the UHR films. This observation suggests that Si is not the unknown pervasive donor in undoped GaN. At this time the identification of the native donor in undoped highly conducting layers is still not definitive. Although a recent positron annihilation study has detected the presence of Ga-vacancies in autodoped n-type films, it does not exclude the presence of other possible native donors [33].

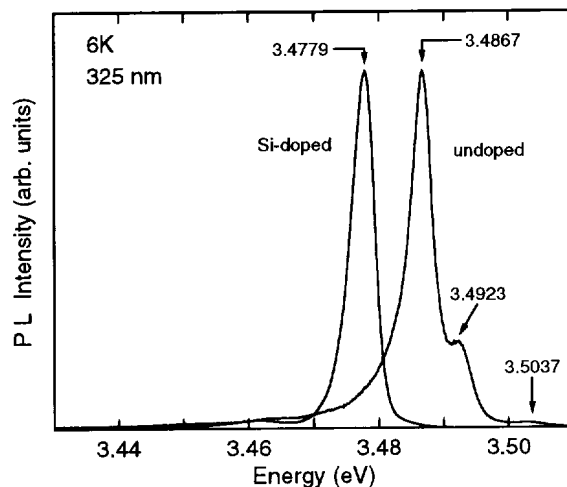


Fig. 5. Normalized edge emission of a UHR and Si-doped GaN films deposited on a-plane sapphire substrates.

V. Donor-acceptor pair emission

Photoluminescence spectra of semiconductors containing substantial amounts of both donors and acceptors can be dominated by recombination processes associated with donor-acceptor pairs (DAP). In the DAP recombination mechanism, electrons bound at neutral donors recombine radiatively with holes bound at neutral acceptors. If a donor and an acceptor are separated by a reasonably short distance, r , they can recombine by emitting a photon with energy $E(r)$ given by [34]

$$E(r) = E_g - (E_D + E_A) + (e^2/\epsilon r) - (e^2/\epsilon)(a^5/r^6),$$

where E_g is the bandgap energy, E_D and E_A are the isolated donor and acceptor binding energies, respectively, ϵ is the static dielectric constant, and a is the effective van der Waals coefficient for the interaction between a neutral donor and a neutral acceptor. For r values much larger than the lattice constant (distant pairs) the discrete emission peaks coalesce into a broad band with the peak position determined largely by the distribution of donor-acceptor pair distances. In the limit of infinite separation (r_∞), the low energy edge of the DAP emission band occurs at a minimum value given by [35]

$$E_{\min} = E_g - (E_D + E_A).$$

Numerous acceptors have been successfully activated in various SiC polytypes [36]. However, Al is the shallowest acceptor in all polytypes. Fig. 6 shows PL spectra of a Al-doped 3C-SiC film measured at two different excitation intensities. At low excitation intensity (spectrum (a), 0.1 mW/cm²) the recombination processes are mostly dominated by distant N-Al pairs due to their longer recombination time. Upon increasing laser excitation intensity, we observe an increasing contribution from the closer N-Al pairs (short lived). Therefore, we should observe an increasing intensity in the high energy side of the DAP PL-band. This behavior is clearly observed in curve (b) of Fig. 6 (1.0 W/cm²). The blue-shift of the spectrum (b) is indicated in Fig. 6 by the dashed lines which mark the peak position of the zero phonon line (ZPL) of the distant DAP band. The sharp lines, magnified in curve (c), are due to the very close pairs, starting from shell number 3, observed only at high excitation conditions due to their very short life time. PL decay spectra taken

at different energy positions of this broad PL-band cannot be characterized by a single exponential, which is typical behavior of DAP recombination processes [37]. Temperature dependence studies of the PL spectra in the close- (sharp-line spectral region) and distant-pairs (DAP-ZPL) yielded values of 257 eV and 54 meV for the Al-acceptor and N-donor binding energy, respectively [29,38]. Note that this N-donor binding energy is in excellent agreement with the value obtained from the IR experiment.

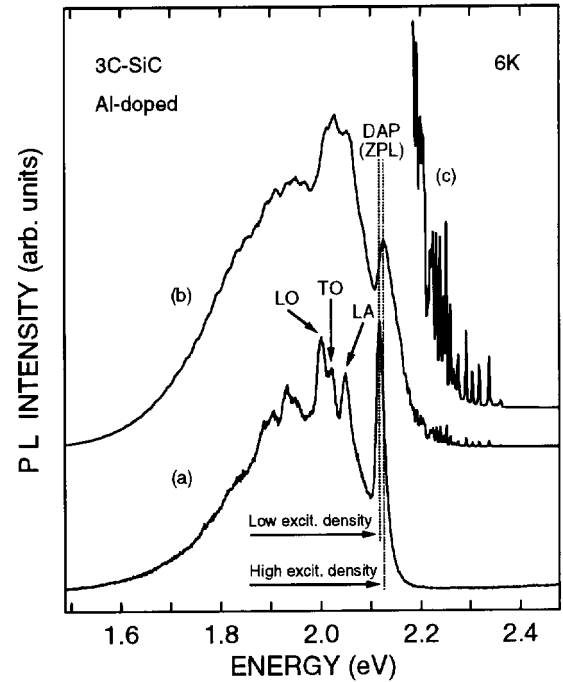


Fig. 6. LTPL spectra of a Al-doped cubic SiC film excited by: (a) 0.1 mW/cm² of 460 nm light from a Xenon lamp-double monochromator, (b) 1 W/cm² of 476.5 nm from an Ar ion laser. (c) Detail of the close-pairs discrete lines.

P-type doping processes in GaN layers are not yet optimized. Although Zn and Mg, the most commonly used p-type dopants, can be incorporated in MOCVD deposited films, its activation usually requires a post-growth treatment [39,40]. Fig. 7 shows the PL spectra of two GaN films doped with the same amount of Mg impurities, but subjected to different thermal annealing conditions. The solid line spectrum is associated with the sample having the lower level of Mg-activation. Note that in addition to the yellow band we observe a dominant blue band between 2.6 and 3.4 eV. This blue band is assigned to a DAP recombination process involving the Mg-acceptors and the unknown donors. This DAP band is characterized by a ZPL at about

3.265 eV and LO- phonon replicas 92 meV apart [41]. This spectrum also shows two small peaks between 3.49 and 3.35 eV. The more intense, at higher energy, is assigned to X-D^o, and the weaker is probably associated with X-Mg^o. The dotted-line spectrum shows no evidence of the yellow emission band or the edge emission. In addition, we observe changes in the line shape (reduction of the ZPL and phonon-replicas line intensities) and red-shift of the DAP band. DAP emission band broadening and red-shift with increasing doping level, in other semiconductor systems, have been attributed to the formation of impurity band [42]. However, in the Nitrides system we cannot disregard the possibility of the formation of Mg- related complexes or clusters [43].

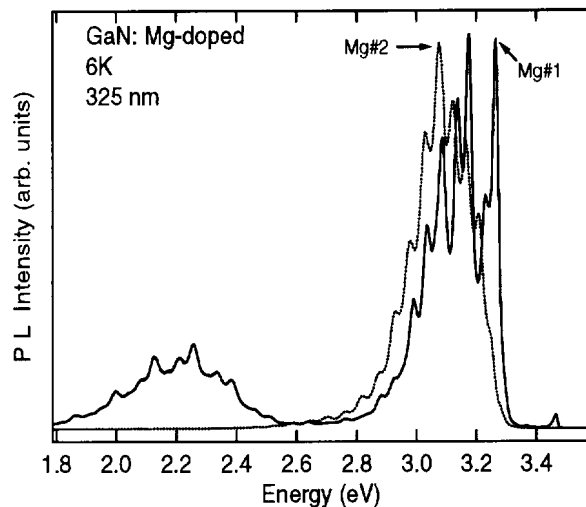


Fig. 7. Normalized PL spectra of Mg-doped samples with different activated Mg levels. Note the modulation of both spectra by interference fringes.

VI. Summary

We have outlined the use of a combination of optical techniques to study the optical and electronic properties of SiC and GaN. Raman scattering was applied to identify the polytype and crystalline quality of heteroepitaxial film and bulk materials. Low temperature PL was employed for both material systems to detect and identify impurities and defects on the basis of their recombination mechanisms. Temperature and excitation intensity studies were used to classify recombination processes and to determine the impurity ionization energies. The IR absorption experiment carried in bulk 3C-SiC yielded the binding energy for native donors in SiC and the value of the valley-orbit splitting.

Acknowledgments

We would like to thank M.A. Khan, K. Doverspike, A.E. Wickenden, P.H. Klein, P.E.R. Nordquist, Jr., V.L. Zuev, and L.M. Ivanova for providing the samples used in these experiments. This work was supported by the Office of Naval Research.

References

- 1 J.A. Lely, Ber. Deut. Keram. Ges. **32**, 229 (1955).
- 2 J.W. Palmour, C.H. Carter, Jr., C.E. Weitzel, and K.J. Nordquist, in *Mat. Res. Soc. Symp. Proc., vol.339, Diamond, SiC and Nitrides Wide Bandgap Semiconductors*, ed. C.H. Carter, Jr., G. Gildenblat, S. Nakamura, and R.J. Nemanich (1994) p. 133.
- 3 V. Shields, K Fekade, and M. Spencer, in *Inst. Phys. Conf. Ser. NO. 137*, ed. M.G. Spencer, R.P. Devaty, J.A. Edmond, M.A. Khan, R. Kaplan, and M. Rahman (1993) p. 21.
- 4 J. Yang, S. Mshino, J.A. Powell, and P. Pirouz, in *Inst. Phys. Conf. Ser. NO. 137*, ed. M.G. Spencer, R.P. Devaty, J.A. Edmond, M.A. Khan, R. Kaplan, and M. Rahman (1993) p. 25.
- 5 M.W. Russel, J.A. Freitas, Jr., W.J. Moore, and J.E. Butler, *Ad. Mat. for Opt. and Elect.* **7**, (1997).
- 6 W.J. Moore, R. Kaplan, J.A. Freitas, Jr., Y.M. Altaiskii, V.L. Zuev, and L.M. Ivanova, in *Mat. Res. Soc. Symp. Proc., vol.339, Diamond, SiC and Nitrides Wide Bandgap Semiconductors*, ed. C.H. Carter, Jr., G. Gildenblat, S. Nakamura, and R.J. Nemanich (1994) p. 717.
- 7 S. Nishino, J.A. Powell, and H.A. Will, *Appl. Phys. Lett.* **42**, 460 (1983).
- 8 H.P Liaw and R.F. Davis, *J. Electrochem. Soc.* **131**, 3014 (1984).
- 9 A. Addamiano and P.H. Klein, *J. Crystal Growth* **70**, 291 (1984).
- 10 B. Segall, S. A. Alterovitz, E. J. Haugland, and L. G. Matus, *Appl. Phys. Lett.* **49**, 450 (1986).
- 11 A. Suzuki, A. Ogura, K. Furukawa, Y. Fujii, M. Shigeta, and S. Nakajima, *J. Appl. Phys.* **64**, 2818 (1988).
- 12 W.J. Moore, *J. Appl. Phys.* **74**, 1805 (1993).
- 13 P. Pirouz, C.M. Chorey, and J.A. Powell, *Appl. Phys. Lett.* **50**, 221 (1987).
- 14 J.A. Powell, L.G. Mattus, M.A. Kuczumski, C.M. Chorey, T.T. Cheng, and P. Pirouz, *Appl. Phys. Lett.* **51**, 823 (1987).

- 15 C.M. Balkas, Z. Sitar, T. Zheleva, L. Bergman, I.K. Shmagin, J.F. Muth, R. Kolbas, R. Nemanich, and R.F. Davis, in *Mat. Res. Soc. Symp. Proc.*, vol. 449, III-V Nitrides, ed. F.A. Ponce, T.D. Moustakas, I. Akasaki, B.A. Monemar (1997) p. 41.
- 16 S. Porowski, M. Bockowski, B. Lucznik, M. Wroblewski, S. Kruwski, I. Grzegory, M. Leszczynski, G. Nowak, K. Pakula, and J.M. Baranowski, in *Mat. Res. Soc. Symp. Proc.*, vol. 449, III-V Nitrides, ed. F.A. Ponce, T.D. Moustakas, I. Akasaki, B.A. Monemar (1997) p. 35.
- 17 J.M. Baranowski, Z. Liliental-Weber, K. Korona, K. Pakula, R. Stepniewski, A. Wyszniak, I. Grzegory, G. Nowak, S. Porowski, B.A. Monemar, and P. Bergman, in *Mat. Res. Soc. Symp. Proc.*, vol. 449, III-V Nitrides, ed. F.A. Ponce, T.D. Moustakas, I. Akasaki, B.A. Monemar (1997) p. 393.
- 18 S.D. Lester, F.A. Ponce, M.G. Craford, and D.A. Steigerwald, *Appl. Phys. Lett.* **66**, 1249 (1995).
- 19 B. Heying, X.H. Wu, S. Keller, Y. Li, D. Kopolnek, B. Keller, S.P. Denbars and J.S. Speck, *Appl. Phys. Lett.* **68**, 643 (1996).
- 20 M.A. Khan, J.N. Kuznia, J.M. Van Hove, and D.T. Olson, *Appl. Phys. Lett.* **58**, 526 (1991).
- 21 M.A. Khan, R.A. Skogman, J.M. Van Hove, D.T. Olson, and J.N. Kuznia *Appl. Phys. Lett.* **60**, 1366 (1992).
- 22 A.E. Wickenden, L.B. Rowland, K. Doverspike, D.K. Gaskil, J.A. Freitas, Jr., D.S. Simons, and P.H. Chi, *J. Electron. Mater.* **24**, 1547 (1995).
- 23 J.A. Freitas, Jr., in *Propert. of Silicon Carbide*, ed. G.L. Harris, Datareviews series (IEEE- inspec) No. 13 (1995) p. 21.
- 24 H. Okumura, K. Balakrishnan, G. Feuillet, K. Ohta, H. Hamaguchi, S. Chichibu, Y. Ishida, and S. Yoshida, in *Mat. Res. Soc. Symp. Proc.*, vol. 449, III-V Nitrides, ed. F.A. Ponce, T.D. Moustakas, I. Akasaki, B.A. Monemar (1997) p. 435.
- 25 J.A. Freitas, Jr., and M.A. Khan, in *Mat. Res. Soc. Symp. Proc.*, vol. 339, *Diamond, SiC and Nitrides Wide Bandgap Semiconductors*, ed. C.H. Carter, Jr., G. Gildenblat, S. Nakamura, and R.J. Nemanich (1994) p. 547.
- 26 W.J. Choyke, *Mat. Res. Bull.* **4**, 5141 (1969).
- 27 W.J. Choyke, D.R. Hamilton, and L. Patrick, *Phys. Rev.* **A1163**, 133 (1964).
- 28 W.J. Moore, R. Kaplan, J.A. Freitas, Jr., Y.M. Altaiskii, V.L. Zuev, and L.M. Ivanova, in *Mat. Res. Soc. Symp. Proc.*, vol. 339, *Diamond, SiC and Nitrides Wide Bandgap Semiconductors*, ed. C.H. Carter, Jr., G. Gildenblat, S. Nakamura, and R.J. Nemanich (1994) p. 717.
- 29 J.A. Freitas, Jr., S.G. Bishop, P.E.R. Norquist, Jr., and M.L. Gipe, *Appl. Phys. Lett.* **52**, 1695 (1988).
- 30 W. J. Moore, J. A. Freitas, Jr., and P. J. Lin-Chung, *Sol. State Commun.* **93**, 389 (1995).
- 31 T. Ogino and M. Aoki, *Jpn. J. Appl. Phys.* **19**, 2395 (1980).
- 32 J.A. Freitas, Jr., K. Doverspike, and A.E. Wickenden, in *Mat. Res. Soc. Symp. Proc.*, vol. 395, *Gallium Nitrides and Related Materials*, ed. F.A. Ponce, R.D. Dupuis, S. Nakamura, and J.A. Edmond (1994) p. 485.
- 33 L.V. Jørgenson, A.C. Kruseman, H. Schut, A. Van Veen, M. Fanciulli, and T.D. Moustakas, in *Mat. Res. Soc. Symp. Proc.*, vol. 449, III-V Nitrides, ed. F.A. Ponce, T.D. Moustakas, I. Akasaki, B.A. Monemar (1997) p. 853.
- 34 J.J. Hopfield, D.G. Thomas, and M. Gershenson, *Phys. Rev. Lett.* **10**, 162 (1963).
- 35 D.G. Thomas, M. Gershenson, and F.A. Trumbore, *Phys. Rev.* **A133**, 269 (1964).
- 36 J.A. Freitas, Jr., in *Propert. of Silicon Carbide*, ed. G.L. Harris, Datareviews series (-inspec) No. 13 (1995) p. 29.
- 37 S.G. Bishop and J.A. Freitas, Jr., *J. Cryst. Growth* **106**, 38 (1990).
- 38 J.A. Freitas, Jr. and S.G. Bishop, *Appl. Phys. Lett.* **55**, 2757 (1989).
- 39 S. Nakamura, N. Iwasa, M. Senoh, and T. Mukai, *Jpn. J. Appl. Phys.* **31**, 1258 (1992).
- 40 M.S. Brant, N.M. Johnson, R.J. Molnar, R. Singh, and T.D. Moustakas, *Appl. Phys. Lett.* **64**, 2264 (1994).
- 41 M. Ilegems and R. Dingles, *J. Appl. Phys.* **44**, 4234 (1973).
- 42 J.I. Pankove, *J. Phys. Soc. (Japan)* **21** (suppl.) 298 (1996).
- 43 J.A. Freitas, Jr., A.E. Wickenden, D.D. Koleske, and M.A. Khan, in *Proc. of the 23rd Int. Conf on Compound Semiconductors*, St. Petersburg, Russia (1996).